

## Metabolic engineering of chloroplasts for artemisinic acid biosynthesis and impact on plant growth

BHAWNA SAXENA<sup>1</sup>, MAYAVAN SUBRAMANIYAN<sup>1</sup>, KARAN MALHOTRA<sup>1</sup>, NEEL SAROVAR BHAVESH<sup>1</sup>,  
SHOBHA DEVI POTLAKAYALA<sup>2</sup> and SHASHI KUMAR<sup>1,\*</sup>

<sup>1</sup>International Centre for Genetic Engineering and Biotechnology, Aruna Asaf Ali Marg, New Delhi 110 067, India

<sup>2</sup>School of Science Engineering and Technology, Penn State Harrisburg, Middletown, PA 17057, USA

\*Corresponding author (Email, [skrhode@icgeb.res.in](mailto:skrhode@icgeb.res.in))

Chloroplasts offer high-level transgene expression and transgene containment due to maternal inheritance, and are ideal hosts for biopharmaceutical biosynthesis via multigene engineering. To exploit these advantages, we have expressed 12 enzymes in chloroplasts for the biosynthesis of artemisinic acid (precursor of artemisinin, antimalarial drug) in an alternative plant system. Integration of transgenes into the tobacco chloroplast genome via homologous recombination was confirmed by molecular analysis, and biosynthesis of artemisinic acid in plant leaf tissues was detected with the help of <sup>13</sup>C NMR and ESI-mass spectrometry. The excess metabolic flux of isopentenyl pyrophosphate generated by an engineered mevalonate pathway was diverted for the biosynthesis of artemisinic acid. However, expression of megatransgenes impacted the growth of the transplastomic plantlets. By combining two exogenous pathways, artemisinic acid was produced in transplastomic plants, which can be improved further using better metabolic engineering strategies for commercially viable yield of desirable isoprenoid products.

[Saxena B, Subramaniyan M, Malhotra K, Bhavesh NS, Potlakayala SD and Kumar S 2014 Metabolic engineering of chloroplasts for artemisinic acid biosynthesis and impact on plant growth. *J. Biosci.* **39** 33–41] DOI 10.1007/s12038-013-9402-z

### 1. Introduction

Artemisinin, a derivative of artemisinic acid (AA), has proven to be incredibly effective in the treatment of malaria, even against different forms of the disease that have developed resistance to previously successful therapies. To maintain artemisinin's effectiveness against this pathogen, the World Health Organization (WHO 2010) strongly recommends its use only in combination with other anti-malarials, known as artemisinin combination therapies (ACTs) (WHO 2001; Davis *et al.* 2005). The high cost of artemisinin-based therapies combined with the low yields of artemisinin from *Artemisia annua* (sweet wormwood), however, have severely limited its large-scale commercialization (Mutabingwa 2005) and, hence, its affordability to the poor (Enserink 2005), who are often the most in need of treatment. The ability to semi-synthetically produce

artemisinin would significantly reduce the cost of artemisinin-based therapies, thereby increasing the affordability of ACTs.

Scientific efforts were made to enhance artemisinin production via plant breeding (White, 2008) as well as through genetic engineering approaches in *A. annua* (Chen *et al.* 2000; Zhang *et al.* 2008), none of which have been successful due to poor plant regeneration and transformation frequency (Vergauwe *et al.* 1996, 1998; Chen *et al.* 2000). Chemical synthesis of artemisinin is even more difficult due to its complex chemical structure (Xu *et al.* 1986; Avery *et al.* 1992).

A less complex molecule than artemisinin, AA can be used as a starting point for obtaining semi-synthetic artemisinin (figure 1). Artemisinic acid is a key substrate for the production of dihydroartemisinic acid (DHAA), which can be converted to artemisinin in the presence of oxygen and light with the help of a photo-bioreactor (Wallaart *et al.* 2000a; Levesque

**Keywords.** Antimalarial drug; artemisinin; gene pyramiding; isopentenyl-diphosphate/isopentenyl pyrophosphate (IPP); metabolic flux; mevalonate (MEV) pathway; plastome; transplastomics

Supplementary materials pertaining to this article are available on the *Journal of Biosciences* Website at <http://www.ias.ac.in/jbiosci/mar2014/supp/Saxena.pdf>

and Seeberger 2012) or plants (Farhi et al. 2011). Artemisinic acid was successfully produced by engineered yeast (Ro et al. 2006) and transformed tobacco plants (Van Herpen et al. 2010). However, use of nuclear transformation of tobacco plants yielded a very low amount of artemisinin (Farhi et al. 2011). To enhance the yield, Farhi et al. (2011) suggested using an alternative expression system like chloroplast transformation, which offers a number of unique advantages including high levels of transgene expression (up to 46.1% total leaf protein), multi-gene expression in a single transformation event, and transgene containment due to maternal inheritance. The ability of chloroplasts to fold proteins correctly for the formation of the proper disulfide bridges, along with the presence of chaperones, are the attractive features for the production of therapeutic proteins in transformed chloroplasts (Kumar et al. 2004; Kumar and Daniell 2004; Daniell et al. 2005). In this investigation, an exogenous cytosolic mevalonate (MEV) pathway (Kumar et al. 2012), along with an AA biosynthesis pathway (figure 1) containing *isopentenyl diphosphate isomerase*, *modified amorpha-4,11-diene synthase*, *A. annua-amorpha-4,11-diene C-12 oxidase* and *A. annua-cytochrome P450 reductase* genes, was introduced into tobacco chloroplasts to generate a flux of carbon towards the formation of isopentenyl-diphosphate (IPP), leading to AA biosynthesis.

## 2. Materials and methods

### 2.1 Construction of the chloroplast transformation vector

The complete AA biosynthesis vector ‘pMEV-Arte’ was designed *in silico*; and synthesized with the help of Biobasic Inc. (Canada). The vector contains the operon encoding the MEV pathway, including the yeast open reading frames (orfs) encoding phosphomevalonate kinase (PMK, ERG8), mevalonate kinase (MVK, ERG12), mevalonate diphosphate decarboxylase (MDD, ERG19), acetoacetyl CoA thiolase (AACT, ERG10), 3-hydroxy-3-methylglutaryl-CoA (HMG-CoA) synthase (HMGS, ERG13), and a C-terminal truncated HMGCoA reductase (HMGRt), as described (Kumar et al. 2012). The AA biosynthesis pathway comprised of *isopentenyl diphosphate isomerase* genes (IPP; gi|4633512) and *farnesyl diphosphate synthase* (FPP; gi|216582) genes from *Escherichia coli*; modified *amorpha-4,11-diene synthase* (SynADS; Anthony et al. 2009), *A. annua* *amorpha-4,11-diene C-12 oxidase* (CYP71AV1, gi|82548247) and *A. annua* *cytochrome P450 reductase* (AACPR, gi|83854016). All the genes, along with DNA sequences for artemisinic acid biosynthesis, were kindly provided by Prof Jay Keasling, University of California, Berkeley, USA. The pMEV-Arte vector (23 kb) contained a total of 12 genes; each gene was engineered with a ribosome-binding site at 5'-end. The 16S-ribosomal rRNA promoter drove the first six genes of the MEV pathway. The remaining six genes of the

AA biosynthesis (including an antibiotic selection marker *aadA*) were driven by *psbA* promoter. The multigene cassette was introduced in between two flanking regions designated as 16S-*trnI* and *trnA*-23S (figure 2A).

### 2.2 Chloroplast transformation and selection

The leaf tissues of *Nicotiana tabacum* cv. Petit Havana SR1 were transformed as described by Kumar and Daniell (2004), using S550d gold particles following the manufacturer's instructions (SeaShell Technology Inc., San Diego, California). Transgenic shoots were recovered on RMOP medium containing 500 mg/L spectinomycin.

### 2.3 Analysis of transgene integration into chloroplast genome

**2.3.1 PCR analysis:** The integration of transgene cassette into transplastomic shoots namely, T1, T2 and T3 was tested by PCR and oligo pair Spec-mF, CGACATTGATCTG GCTATCTTGCTGACA, and 23S-R, ATTACTACG CCCTTCCTCGTCTCTGGG (Sigma Life Science, Bangalore, India). The Spec-mF was designed to bind to the internal region of the *aadA* transgene while 23S-R binds to the native chloroplast genome (23S-rRNA), beyond the homologous recombination site of right flank (*trnA*) (figure 2A–B).

**2.3.2 Southern blot analysis:** For the confirmation of stable transgene integration into transplastomic shoots T1 and T3, about 2 µg genomic DNA of transgenics and wild-type tissues (isolated by DNeasy Plant Mini Kit, Qiagen) were digested with *SphI* and electrophoresed on a 0.8% agarose gel. DNA from the gel was transferred to nitrocellulose membrane and probed with P<sup>32</sup>-radiolabelled *aadA* gene fragment (0.84 kb, obtained from pMEV-Arte vector with *SphI* and *SalI* digestion; as indicated in figure 2A), and Southern blot was developed following the protocol of Kumar and Daniell (2004).

### 2.4 Analysis of artemisinic acid biosynthesis in transgenics

**2.4.1 Extraction of AA from transgenics:** The transplastomic leaf tissues (stored in –80°C) were used for the extraction of AA. Transgenic leaf tissue (1.0 g) was ground in liquid nitrogen. 5 mL of ethyl acetate was added to the ground tissue and vigorously mixed before centrifugation at 5000g at 4°C for 15 min. The ethyl-acetate was evaporated and methanol was added to the crude extract. This mixture was incubated overnight on a rotatory shaker at 37°C at a speed of 160 rpm. After centrifugation, the supernatant was transferred to a fresh tube and analyzed by electrospray ionization

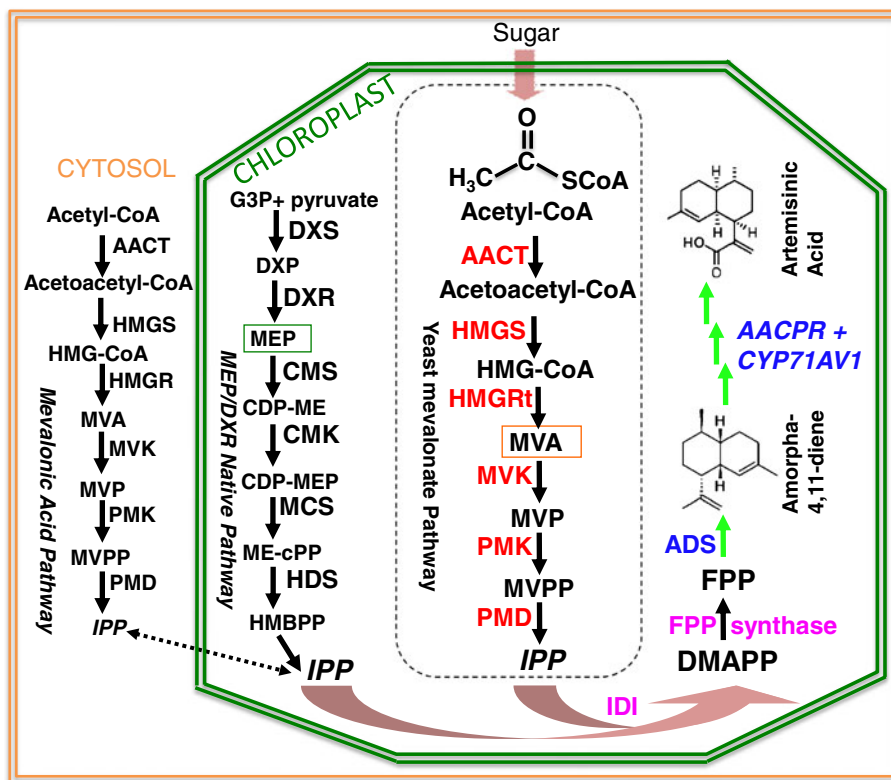


**Figure 1.** Overview of artemisinin acid (AA) biosynthesis in tobacco chloroplasts via multigene engineering. The up-regulated six mevalonate (MEV) pathway enzymes engineered from *Saccharomyces cerevisiae* (shown in red font, in a dotted box) were used to generate excess IPP pool for AA biosynthesis. Two enzymes (in purple font) isopentenyl diphosphate isomerase (IDI) and farnesyl diphosphate (FPP or ispA) synthase, were cloned from *Escherichia coli*. Three transgenes (marked with blue color) encoding amorpha-4, 11-diene, and AA biosynthesis were cloned from *Artemisia annua* L. A green arrow indicates the biochemical pathway leading from farnesyl pyrophosphate (FPP) to amorpha-4,11-diene biosynthesis. The three overlapping green arrows indicate the three-steps of oxidation of amorpha-4,11-diene to AA biosynthesis, which is catalyzed by the multifunctional cytochrome P450 enzyme, CYP71AV1 (also known as amorphadiene oxidase or AMO), in association of reductase, AACPR (*A. annua* cytochrome P450 reductase). Enzymes shown in colored fonts (red, purple and blue) are the only transgenes engineered into tobacco chloroplast genome for the biosynthesis of AA.

(ESI) mass spectrometry. Methanol was evaporated using rotary evaporator (vacuo) and deuterated methanol was added for  $^{13}\text{C}$  nuclear magnetic resonance (NMR) analysis.

**2.4.2 NMR analysis:** One-dimensional  $^{13}\text{C}$  NMR spectra were measured at  $25^\circ\text{C}$  on a Bruker Avance III spectrometer equipped with a cryogenic triple-resonance TCI probe head, operating at a field strength of 500.13 MHz. The structural identification of AA as a reference compound was based on 1D  $^{13}\text{C}$  spectra. Crude extracts from wild-type and transformed tissues were extracted through ethyl acetate extraction method and subjected to  $^{13}\text{C}$  NMR spectroscopy. All the spectra were measured by dissolving the standard pure AA (Apin Chemicals, UK) and extracts in  $\text{d}_4$ -Methanol (figure 3A–B). All the  $^{13}\text{C}$  resonances of AA were observed in the 1D  $^{13}\text{C}$  spectra of crude extract. Using the earlier reported assignments of standard pure AA;  $^{13}\text{C}$  resonances

were identified and marked in the spectrum (Misra *et al.* 1993; Van Herpen *et al.* 2010). (Atom numbers are referred to in supplementary figure 2 and supplementary table 1).

**2.4.3 ESI-mass spectrometry and GC-MS analysis:** About 2 mL pure AA standard (Apin Chemicals, UK) prepared in methanol solvent (1 mg/ml) was injected into a Synapt GZ high-definition mass spectrophotometer (Waters Corporation, US) using a spray needle. The voltage was set to 2.5 KV while the ion transfer capillary temperature was set at  $220^\circ\text{C}$ . The ion trap contained helium as a damping gas and the auxiliary gas flow rate was set to five arbitrary units. The full scan spectrum was obtained in the range of  $m/z$  150 to 800. The data was acquired in negative ion mode and strongest peak was observed at  $m/z$  233.02 due to AA ( $\text{C}_{15}\text{H}_{22}\text{O}_2$ ; molecular weight as 234.33) with  $[\text{M}-\text{H}]^-$ . Using the same parameters, a full scan of the wild-type

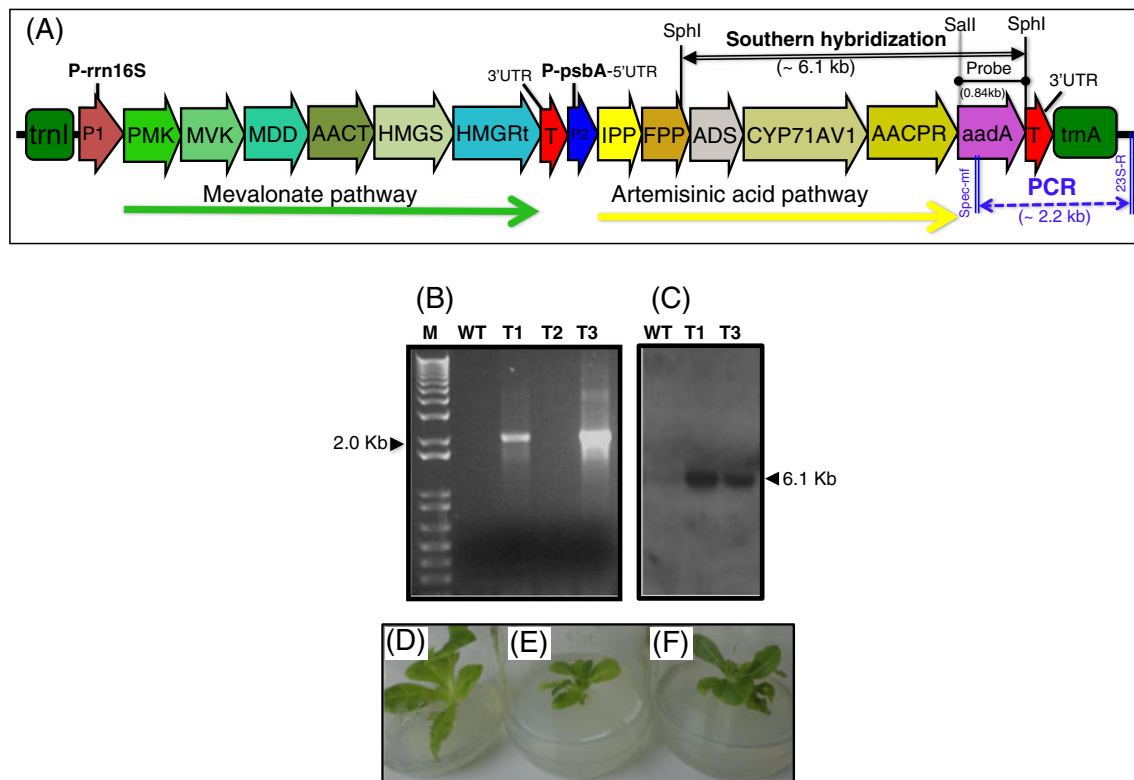


**Figure 2.** Analysis of transgenes integration of isoprenoid and AA biosynthesis pathways into tobacco chloroplast genome and impact of these transgenes on plant growth. (A) Physical map of the chloroplast specific transformation vector ‘pMEV-Arte’ (not to scale) containing right (*trnI*) and left (*trnA*) flanks, used for the homologous recombination transgene cassette into the chloroplast genome. The transgene cassette containing cytosolic MEV (8167 bp) and AA biosynthesis (6848 bp) pathways was positioned in between the left and right flanks. The black line over the vector-map denotes the location of Southern hybridization for confirming integration of transgenes into the chloroplast genome. The blue dotted line represents the PCR amplification of integrated transgenes and corresponding vertical double lines indicate the annealing sites of the internal and external primers (B) The PCR amplicon ~2.2 kb is produced in transgenics T1 and T3 with primer set Spec-m-F (binds to *aadA* transgene) and 23S-R (binds outside the homologous recombination site of native chloroplast genome). No PCR amplification was observed in transgenic T2 (mutant line) and wild-type plant. (C) For Southern blot analysis, genomic DNA (~2 µg) from wild-type and transgenic plant (T1 and T3) samples was digested with *SphI*. DNA transferred to nitrocellulose membrane was hybridized with  $p^{32}$ -labelled *aadA* probe (0.84 kb) and 6.1 kb fragment was observed on an autoradiogram, confirming the transgene integration into the chloroplast genome of T1 and T3. (Note: a faint band in wild-type (WT) is due to DNA leakage from T1 well). (D) Morphological phenotypes of wild-type compared to transplastomic plantlets. (E) Transplastomic T1 and (F) Transplastomic T3 plantlets, undersized in growth, compared to *in vitro* grown wild-type plant after 6 weeks.

samples was obtained with and without the addition of 0.1 mg/mL of AA as a control, and the spectra were compared with transgenic samples.

The fresh transplastomic leaf tissue (1.0 g) of T1 transgenic plant was ground in liquid nitrogen, mixed in 2 mL ethyl acetate and sonicated for 10 min. After 15 min of centrifugation at 5000 rpm, the supernatant was transferred to a new vial, where the solvent was evaporated using rotary evaporator, and the final residue was dissolved in 1 mL of methanol. Samples were analysed by GC-MS using the vendor’s facility (Shimadzu QP-1020 Gas Chromatograph Mass Spectrometer at AIRF, JNU, New Delhi). For quantification, 1 µL was injected into the column and the temperature was increased

as reported (Van Herpen *et al.* 2010). Standard AA (Apin Chemicals, U.K.) was used as reference.

### 3. Results

#### 3.1 Chloroplast transformation

The chloroplast transformation vector pMEV-Arte (figure 2A), containing multigenes of the cytosolic mevalonate pathway (Kumar *et al.* 2012) and the AA biosynthesis pathway (Martin *et al.* 2003; Withers *et al.* 2007), was inserted at the *trnI* and *trnA* chloroplast regions via

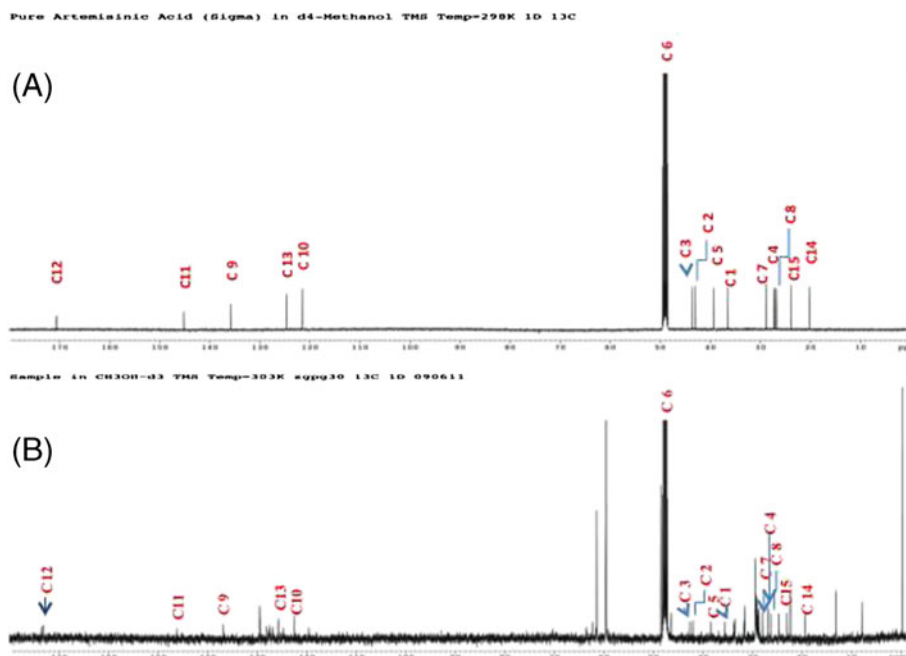


**Figure 3.** One-dimensional  $^{13}\text{C}$  NMR Spectra of (A) The spectrum of pure AA (Apin Chemicals, UK) was used as control (B) The spectrum of AA metabolite; isolated from the transplastomic tissues (T1) was observed similar to the profile of pure AA. Structure of AA and atom numbers are referred to in this figure can be found in supplementary table 1 and supplementary figure 2. All spectra were measured using  $\text{d}_4$ -methanol as solvent.

homologous recombination. The transgenic tissues were selected using antibiotic resistant gene *aadA* (Svab and Maliga 1993) driven by light regulated promoter *psbA*. After 7 weeks of bombardment of the tobacco leaf explants, three independent transgenic shoots, namely, T1, T2 and T3, were recovered on RMOP medium supplemented with 500 mg/L spectinomycin.

### 3.2 Analysis of transgene integration

The integration of all transgenes was initially screened using different sets of gene specific primers. The oligo ‘Spec-mF’ (which anneals to the coding region of *aadA*) and ‘23S-R’ (which binds to native chloroplast genome, beyond the homologous recombination site of *trnA*) were used to ensure transgenes integration specifically into the plastome at *trnI* and *trnA* sites, as indicated by the dotted blue line in figure 2A. Three independent transplastomic shoots surviving on spectinomycin selection medium were tested for PCR and two of them (T1 and T3) were PCR positive as represented by the expected ~2.2 kb amplicon (figure 2B). No PCR amplification observed in the T2 putative transformant, in spite of the plant growing well on spectinomycin supplemented growth medium.

Transgenes integration into the tobacco plastomes of T1 and T3 shoots was further confirmed by Southern blot analysis. The expected integration of ~6.1 kb was spotted on the autoradiogram when transplastomic genomic DNA was hybridized with a  $\text{P}^{32}$ -radiolabelled probe (*aadA* gene), as indicated by a double-line black arrow in figure 2A. Therefore, the true integration of pMEV-Arte cassette into the plastomes of T1 and T3 transgenics was confirmed (figure 2C).

### 3.3 Analysis of artemisinin acid biosynthesis in transgenics

The overview of multigene engineering of MEV and AA biosynthesis pathway into tobacco chloroplasts is shown in figure 1. Six enzymes of MEV pathway from the *Saccharomyces cerevisiae* (in red font) were engineered into tobacco chloroplasts to generate excess IPP pool. Transgenes isopentenyl diphosphate isomerase (IDI) and farnesyl diphosphate (FPP or ispA) synthase (in purple font) from *Escherichia coli* were introduced to convert IPP into dimethylallyl pyrophosphate (DMAPP) and Farnesyl pyrophosphate (FPP) intermediates respectively. Last three key enzymes, encoding amorpha-4,11-diene synthase (ADS), cytochrome P450

monooxygenase (CYP71AV1) *A. annua* cytochrome P450 reductase (AACPR) from *A. annua* were engineered into chloroplasts for AA biosynthesis (marked with blue font). A green single arrow indicates the conversion of FPP to amorpha-4,11-diene, and group of three arrows symbolized three-steps of oxidation of amorpha-4,11-diene to AA, catalyzed by the multifunctional cytochrome P450 enzyme, CYP71AV1, in association with AACPR (*A. annua* cytochrome P450 reductase). The transgenes, which are denoted with colored fonts, were introduced into the tobacco chloroplast genome for AA (precursor to artemisinin) biosynthesis (figure 1).

The AA biosynthesis in transplastomic leaf tissues was analyzed via  $^{13}\text{C}$  NMR and ESI mass spectrometry. For NMR analysis, extracted samples of wild-type and transplastomic tissues were subjected to one-dimensional  $^{13}\text{C}$  NMR analysis. A  $^{13}\text{C}$  chemical shift was observed in the region of 7–180 ppm in the extracted mixture. Comparison to an original standard of AA, with data available in literature (Misra et al. 1993; Van Herpen et al. 2010), was used to assign resonances to AA extracted from transplastomic cultures. The overlap of the observed resonances of AA extracted from the transplastomic samples was very similar to the reference AA profile, with only minor differences due to the presence of native plant metabolites (figure 3A–B).

For ESI-mass spectrometry, a full scan of pure AA was obtained to compare with the wild-type and transgenic samples. A strong AA peak was observed at  $m/z$  233.02 in the wild-type samples, only when spiked in with pure AA (figure 4A). A similar peak was also observed at  $m/z$  233.02 in transgenic samples (figure 4B). The full scan pattern of pure AA standard (Apin Chemicals, U.K.) is provided in the supplementary material for reference (supplementary figure 1A). No peak for AA biosynthesis was observed in untransformed control plants (supplementary figure 1B). Thus, AA biosynthesis was confirmed with negative ESI-mass spectrometric (MS)  $m/z$  spectra in transplastomics. The expression of the MEV and AA pathways in tobacco chloroplasts produced about 0.1 mg/g-FW AA, quantified using GC-MS and standard AA.

### 3.4 Influence of megagene on transgenic phenotype

Out of 50 bombardment events, two positive transplastomic shoots (T1 and T3) were recovered under low light conditions (~100 lux) using chloroplast specific megagene vector 'pMEV-Arte'. The transplastomic cultures grew at a slower rate than wild-type *in vitro* control plants (figure 2D–F). Morphologically, they were stunted in growth and failed to induce proper root fibres after three repetitive cycles of regeneration, which were performed to induce the homoplasmic state in transplastomic plants.

## 4. Discussion

A shrub *Artemisia annua* produces artemisinin, which is a potent antimalarial drug. Due to shortage of plant-derived artemisinin and high prices, an alternative source of affordable artemisinin is required (Paddon et al. 2013). The plant-based systems potentially provide a low-cost alternative for the production of biopharmaceuticals. Therefore, for the biosynthesis of AA (precursor to artemisinin), we have explored the chloroplast engineering that has demonstrated successful production of pharmaceuticals and biomaterials (Daniell et al. 2005). In previous studies, IPP derived from native 2-C-methyl-D-erythritol-4-phosphate (MEP) pathways (of chloroplasts) failed to yield enough amorpha-4,11-diene (precursor to AA) in plants (Wu et al. 2006). Further, without generating an extra pool of IPP, Farhi et al. (2011) also reported a low quantity of artemisinin biosynthesis in transformed tobacco plants. Previously, using chloroplast engineering, we have reported a proficient expression of an exogenous MEV pathway involving six enzymes and yielding high IPP levels into chloroplasts that has not perturbed the growth of transplastomic tobacco plants (Kumar et al. 2012). To extend this research further in a fruitful way, we generated the transplastomic plants expressing both cytosolic MEV and AA biosynthesis pathway, so that excess metabolic flux of IPP generated due to expression of MEV pathway can be utilized for AA biosynthesis (figure 1). The successful production of AA can be chemically synthesized into artemisinin (Paddon et al. 2013).

Transformation frequency using megagene vector 'pMEV-Arte' (figure 2A), however, was significantly poor. Out of 50 bombardment events, only two transgenics were recovered, both with stunted growth in comparison to wild-type plants (figure 2D–F). Nevertheless, transgenes integration into plastome via homologous recombination is highly site-specific, devoid of illegitimate recombination. This is contrary to nuclear genome transformation that leads to transgene silencing and variable levels of transgene expression. Therefore, all the transplastomic lines provide a similar level of transgene expression (Dufourmantel et al. 2005). Using a biolistic approach for gene delivery, incorrect transgene integration may also occur in the nuclear genome instead of the chloroplast genome. Since chloroplastic promoters are not functional in the nuclear genome (Eckardt 2006), such transgenics should not produce the desired metabolite, i.e. AA, which was confirmed by NMR and mass spectrometry.

The use of a specific set of primers (Spec-mF and 23S-R bind DNA region beyond the homologous recombination site of right flank) confirmed the true integration of transgenes in the plastome at the specific site of *trnI* and *trnA* and omitted the possibility of a self-replicating vector into chloroplasts. A putative transformant number T2 did not amplify any PCR product (figure 2B), although it grew well

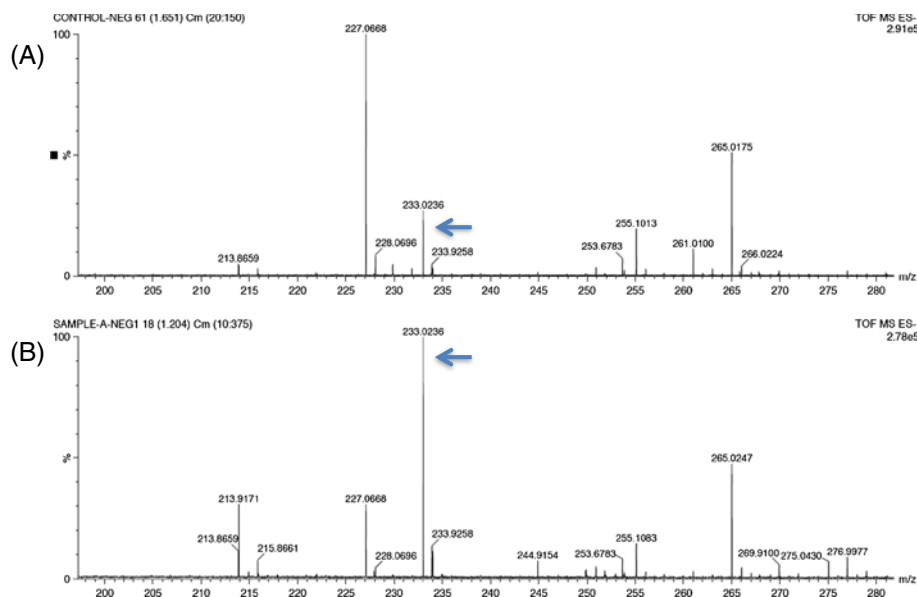


**Figure 4.** TOF-Negative Electrospray Ionization (ESI) Mass spectrometric (MS)  $m/z$  spectra for AA in wild-type and transplastomic (T1) samples, marked with blue arrows. **(A)** An AA peak was observed in wild-type control samples when pure AA was spiked in with minor quantity. **(B)** A dominant mass peak at  $m/z$  233.02 of AA was observed in extract of transplastomic (T1) tissues. The full scan of pure AA and wild-type control extract is shown in supplementary figure 1.

on spectinomycin containing medium, which indicates that specific point mutations in the 16S-rRNA gene, might have allowed the T2 plantlets to confer resistance to spectinomycin (Harris *et al.* 1989). Chloroplasts are highly polyploid in nature. To produce higher amounts of the desired product, transgene integration in the plastome should be in a homoplasmic state, which is persuaded by additional rounds of regeneration and selection (4–8 times) of tissues on a stringent, antibiotic-supplemented medium. This indicates that our transplastomic shoots (T1 and T3) were not in a homoplasmic state; their growth was further subdued after the second and third rounds of selection. The hetroplasmic state of the transformed plastome may be a reason for the low yield of AA biosynthesis in transplastomic plant cells. By combining the two exogenous pathways, about 0.1 mg/g-FW of AA was produced in transplastomic leaf tissues. This yield was low compared to genetically modified yeast (Ro *et al.* 2006), but observed equivalent to the average levels as observed in the yields of *A. annua* (Gupta *et al.* 1996; Wallaart *et al.* 2000b). However, there is a huge variation of AA production in *A. annua* (~0.01–0.2 mg/g-FW), and this is known to be dependent on seasonal changes, geographic origins and stress conditions (Gupta *et al.* 1996; Wallaart *et al.* 2000b). The low yield of AA in our transplastomic plantlets may also be attributed to an insufficient pool of the available acetyl-CoA precursor needed for the IPP biosynthesis. Insufficient levels of acetyl-CoA can impact plant growth and photosynthesis rate (Lössl *et al.* 2003). Previously, Lössl *et al.* (2003) had reported stunted

male sterile plants when three polyester synthesis genes were overexpressed in tobacco chloroplasts. The stunted growth signifies that chloroplasts may be intolerant to excess load of transgenes or due to their nature, which could impact plant growth (figure 2D–F). In evolutionary trends, chloroplast organelles have been observed to either lose unwanted genes or move them into the nuclear genome (Fuentes *et al.* 2012). However, chloroplast transformation is now well established with the time, and this process has been successfully used for expressing multigene MEV pathway (Kumar *et al.* 2012), vitamin E biosynthesis pathway (Lu *et al.* 2013) and production of proinsulin (Boyhan and Daniell 2011), due to higher expression of enzymes when compared to nuclear transformation, and transgenes are largely excluded from pollen transmission (Kumar *et al.* 2004).

In this study, two pathways (MEV from yeast and AA from *A. annua*), whose enzymes are listed in the materials and methods section and in figures 1 and 2, were engineered into tobacco chloroplasts. This combination of pathways has facilitated the biosynthesis of AA in an alternative plants system. Previously, we had reported the RNA expression of individual transgenes related to MEV-pathway expression in tobacco chloroplast using RT-PCR (Kumar, *et al.* 2012). However, we were not able to carry the RNA-based RT-PCR for an additionally engineered AA-pathway due to shortage of leaf material produced from the stunted transplastomics; therefore, our  $^{13}\text{C}$  NMR and ESI-MS studies were focused on the quantification of the final product (AA). Furthermore, quantification of RNA expression levels may not be necessary; that protein will also be

produced/expressed in the same proportion. The weak correlations may be due to various post-transcriptional processes that can complicate attempts to obtain accurate estimates of quantities of corresponding mRNAs destined for translation (Gry *et al.* 2009; Vogel and Marcotte 2012). It may be difficult to decipher an individual expression of metabolites expressed in chloroplasts using the proteomic approach, as native MEV/MEP-pathways already exist in plant systems. Further, in order to test the expression levels by Western blot analysis, our study would have been elaborate and expensive to raise antibodies against all individual transgenes. Also, existence of enzymes as a result of native pathway would have interfered with the prediction of accurate expression levels of individual transgenes.

From an economic point of view, having a high yield of desired product in plant cells is essential. Optimizing pathway flux and balancing intermediates of metabolic pathways in a cell are important factors that need to be addressed to get maximal yields. Further, to make our study more cost-effective, we are interested in engineering tobacco plants with artemisinin biosynthesis pathway using lesser number of transgenes in order to reduce the gene load on plant. Our approach would be to employ transformation of both nuclear and chloroplast genomes using the essential genes for artemisinin production but still making sure to obtain normal plants with no physiological aberrations. The production of isoprenoid-based medicines should be possible through the use of better metabolic engineering strategies and modulation of transgene expression. Strategies, like synthetic biology and modulation of transgenes expression in bacterial and yeast systems, have been very productive (Paddon *et al.* 2013). However, plants are more complex; the genome sequences and networking of all metabolic pathways are not fully deciphered, therefore *in-silico*-based modeling of transgenes regulation in plant system may not provide complete coherence with *in vivo* studies. With an advancement of research, such approaches in future may lead to successful, commercially viable yields of desirable isoprenoid products and provide a consistent, reliable and low-cost supplementary source of drugs for ACTs that are needed for antimalarial treatment. The abundant production of high quality artemisinin from transgenic plants will have a greater impact on malaria mortality along with other benefits, including low startup costs, high flexibility in terms of scale and storage, and the potential to produce high product volumes at a relatively lower cost.

### Acknowledgements

We thank the Department of Biotechnology (DBT) and Department of Science and Technology, India, for providing financial support to SK (grants BT/HRD/35/02/09/2008, BT/PR13028/PID/06/473/2009 and SR/SO/BB-37/2010 respectively). We also like to thank DBT for the grant to NSB for the 500 MHz NMR spectrometers at the ICGEB, New Delhi.

Our sincere thanks to Dr Ranjan Nanda (ICGEB, New Delhi) for his help with the analysis of ESI-mass spectrometry data.

### References

- Anthony JR, Anthony LC, Nowroozi F, Kwon G, Newman JD and Keasling JD 2009 Optimization of the mevalonate-based isoprenoid biosynthetic pathway in *E. coli* for production of the anti-malarial drug precursor amorpha-4,11-diene. *Metab. Eng.* **11** 13–19
- Avery MA, Chong WKM and Jennings-White C 1992 Stereoselective total synthesis of (+)-Artemisinin, the antimalarial constituent of *Artemisia annua* L. *J. Med. Chem.* **114** 974–979
- Boyhan D and Daniell H 2011 Low-cost production of proinsulin in tobacco and lettuce chloroplasts for injectable or oral delivery of functional insulin and C-peptide. *Plant Biotechnol. J.* **9** 585–598
- Chen DH, Ye HC and Li GF 2000 Expression of a chimeric farnesyl diphosphate synthase gene in *Artemisia annua* L. transgenic plants via *Agrobacterium tumefaciens*-mediated transformation. *Plant Sci.* **155** 179–185
- Daniell H, Chebolu S, Kumar S, Singleton M and Falconer R 2005 Chloroplast-derived vaccine antigens and other therapeutic proteins. *Vaccine* **23** 1779–1783
- Davis TME, Karunajeewa HA and Kenneth F 2005 Artemisinin-based combination therapies for uncomplicated malaria. *Ilett. Med. J. Aust.* **182** 181–185
- Dufourmantel N, Tissot G, Goutorbe F, Garçon F, Muhr C, Jansens S, Pelissier B, Peltier G and Dubald M 2005 Generation and analysis of soybean plastid transformants expressing *Bacillus thuringiensis* Cry1Ab protoxin. *Plant Mol. Biol.* **58** 659–668
- Eckardt NA 2006 Genomic hopscotch: Gene transfer from plastid to nucleus. *Plant Cell* **18** 2865–2867
- Enserink M 2005 Infectious diseases: Source of new hope against malaria is in short supply. *Science* **307** 33
- Farhi M, Marhevka E, Ben-Ari J, Dimantov AA, Liang Z, Zeevi V, Edelbaum O, Spitzer-Rimon B, *et al.* 2011 Generation of the potent anti-malarial drug artemisinin in tobacco. *Nat. Biotech.* **29** 1072–1074
- Fuentes I, Karcher D and Bock R 2012 Experimental reconstruction of the functional transfer of intron-containing plastid genes to the nucleus. *Curr. Biol.* **22** 763–771
- Gupta MM, Jain DC, Mathur AK, Singh AK, Verma RK and Kumar S 1996 Isolation of a high artemisinic acid containing plant of *Artemisia annua*. *Planta Med.* **62** 280–281
- Gry M, Rimini R, Stromberg S, Asplund A, Ponten F, Uhlen M and Nilsson P 2009 Correlations between RNA and protein expression profiles in 23 human cell lines. *BMC Genomics* **10** 365
- Harris EH, Burkhardt BD, Gillham WW and Boynton JE 1989 Antibiotic resistance mutations in the chloroplast 16S and 23S rRNA genes of *Chlamydomonas reinhardtii*: correlation of genetic and physical maps of the chloroplast genome. *Genetics* **123** 281–292
- Kumar S, Dhingra A and Daniell H 2004 Plastid-expressed betaine aldehyde dehydrogenase gene in carrot cultured cells, roots, and leaves confers enhanced salt tolerance. *Plant Physiol.* **136** 2843–2854
- Kumar S and Daniell H 2004 Engineering the chloroplast genome for hyperexpression of human therapeutic proteins and vaccine antigens. *Methods Mol. Biol.* **267** 365–384

- Kumar S, Hahn FM, Baidoo E, Kahlon TS, Wood, DF, McMahan CM, Cornish K, Keasling JK, Daniell H and Whalen MC 2012 Remodeling the isoprenoid pathway in tobacco by expressing the cytoplasmic mevalonate pathway in chloroplasts. *Metab. Eng.* **14** 19–28
- Levesque F and Seeberger PH 2012 Continuous flow synthesis of the antimalarial drug artemisinin. *Angew. Chem. Int. Ed.* **51** 1706–1709
- Lössl A, Eibl C, Harloff HJ, Jung C, Koop HU 2003 Polyester synthesis in transplastomic tobacco (*Nicotiana tabacum* L.): Significant contents of polyhydroxybutyrate are associated with growth reduction. *Plant Cell Rep.* **9** 891–899
- Lu Y, Rijzaani H, Karcher D, Ruf S and Bock R 2013 Efficient metabolic pathway engineering in transgenic tobacco and tomato plastids with synthetic multigene operons. *Proc. Natl. Acad. Sci. USA* **110** E623–E632
- Martin V JJ, Pitera DJ, Withers ST, Newman JN and Keasling JD 2003 Engineering a mevalonate pathway in *Escherichia coli* for production of terpenoids. *Nat. Biotech.* **21** 796–802
- Misra LN, Ahmad A, Thakur RS, Lotter H and Wagner H 1993 Crystal structure of artemisinic acid: A possible biogenetic precursor of antimalarial artemisinin from *Artemisia annua*. *J Nat Prod.* **56**(2) 215–219
- Mutabingwa TK 2005 Artemisinin-based combination therapies (ACTs) best hope for malaria treatment but inaccessible to the needy. *Acta Tropica* **95** 305–315
- Paddon C J, Westfall P J, Pitera D J, Benjamin K, Fisher K, McPhee D, Leavell M D, Tai A, et al. 2013 High-level semi-synthetic production of the potent antimalarial artemisinin. *Nature* **496** 528–532
- Ro DK, Paradise EM, Ouellet M, Fisher KJ, Newman KL, Ndungu JM, Ho KA, Eachus RA, et al. 2006 Production of the antimalarial drug precursor artemisinic acid in engineered yeast. *Nature* **440** 940–943
- Svab Z and Maliga P 1993 High-frequency plastid transformation in tobacco by selection for a chimeric *aadA* gene. *Proc. Natl. Acad. Sci. USA* **90** 913–917
- Van Herpen TWJW, Cankar K, Nogueira M, Bosch D, Bouwmeester HJ and Beekwilder J 2010 *Nicotiana benthamiana* as a Production Platform for Artemisinin Precursors. *PLoS ONE* **5** e14222 doi:10.1371/journal.pone.0014222
- Vergauwe A, Cammaert R, Vandenberghe D, Genetello C, Inze´ D, Van Montagu M and Van den Eeckhout E 1996 *Agrobacterium tumefaciens*-mediated transformation of *Artemisia annua* L. and regeneration of transgenic plants. *Plant Cell Rep.* **15** 929–933
- Vergauwe A, Van Geldre E, Inze D, Van Montagu M and Van den Eeckhout E 1998 Factors influencing *Agrobacterium tumefaciens*-mediated transformation of *Artemisia annua* L. *Plant Cell Rep.* **18** 105–110
- Vogel C and Marcotte EM 2012 Insights into the regulation of protein abundance from proteomic and transcriptomic analyses. *Nat. Rev. Genet.* **13** 227–232
- Wallaart TE, Pras N and Quax WJ 2000a Seasonal variations of artemisinin and its biosynthetic precursors in tetraploid *Artemisia annua* plants compared with the diploid wild-type. *Planta* **66** 57–62
- Wallaart TE, Pras N, Beekman AC and Quax WJ 2000b Seasonal variation of artemisinin and its biosynthetic precursors in plants of *Artemisia annua* of different geographical origin: proof for the existence of chemotypes. *Planta Med.* **66** 57–62
- White NJ 2008 Qinghaosu (Artemisinin): The price of success. *Science* **320** 330–334
- World Health Organization 2001 Antimalarial drug combination therapy: report of a WHO technical consultation. WHO/CDS/RBM/2001/35 reiterated in 2003
- Withers ST, Gottlieb SS, Lieu B, Newman JD and Keasling JD 2007 Identification of isopentenol biosynthetic genes from *Bacillus subtilis* using isoprenoid precursor toxicity. *Appl. Environ. Microbiol.* **73** 6277–6283
- World Health Organization 2010 *World malaria report 2010* (WHO, Geneva)
- Wu S, Schalk M, Clark A, Miles RB, Coates R and Chappell J 2006 Redirection of cytosolic or plastidic isoprenoid precursors elevates terpene production in plants. *Nat. Biotechnol.* **24** 1441–1447
- Xu XX, Zhu J, Huang D and Zhou W 1986 Total synthesis of arteannuin and deoxyarteannuin. *Tetrahedron* **42** 819–828
- Zhang Y, Teoh KH, Reed DW, Maes L, Goossens A, Olson DJ, Ross AR and Covello PS 2008 The molecular cloning of artemisinic aldehyde Delta11(13) reductase and its role in glandular trichome-dependent biosynthesis of artemisinin in *Artemisia annua*. *J. Biol. Chem.* **283** 21501–21508

MS received 23 October 2013; accepted 25 October 2013

Corresponding editor: MARÍA LUZ CÁRDENAS